

POLITECNICO DI MILANO  
SPACECRAFT ATTITUDE AND DYNAMICS  
GROUP 75, A.Y. 2021/22

---

## Ocean Cleanup Satellite: ship tracking over the Pacific Garbage Patch

---



07/01 2022

MADS LARSEN [10833041, 984967] FEDERICO INFANTINO [10808187,  
996989] GLORIA CASTRONOVO [10837697, 992130] ALESSANDRO DEL BONO  
[10531050, 993719]



**POLITECNICO**  
MILANO 1863

# Contents

---

<b>Contents</b>	<b>ii</b>
<b>1 Ocean Cleanup Satellite</b>	<b>1</b>
1.1 Overview of the Mission . . . . .	1
1.2 Orbit characterization . . . . .	1
1.3 Spacecraft properties . . . . .	2
1.4 Environment . . . . .	3
1.5 Dynamics . . . . .	5
1.6 Kinematics . . . . .	5
1.7 Sensors . . . . .	6
1.8 Actuators . . . . .	8
1.9 Control . . . . .	10
1.10 Control verification . . . . .	14
1.11 Conclusion . . . . .	16
<b>Bibliography</b>	<b>17</b>
Websites . . . . .	17

# Ocean Cleanup Satellite

1

## 1.1 Overview of the Mission

The Ocean Cleanup is a nonprofit engineering environmental organization based in the Netherlands, that develops technology to extract plastic pollution from the oceans especially focused on the biggest garbage patch in the world, located in the North Pacific Ocean. It is based on a floating structure carried by ships that follow the path of the garbage in the ocean. Our aim is to model a satellite that keeps tracking of the ships in order to build the evolution of the path of the garbage patch and also to monitor with a great field of view the cleaning operations.

For completing this mission the following Attitude determination and control system (ADCS) will be implimented.

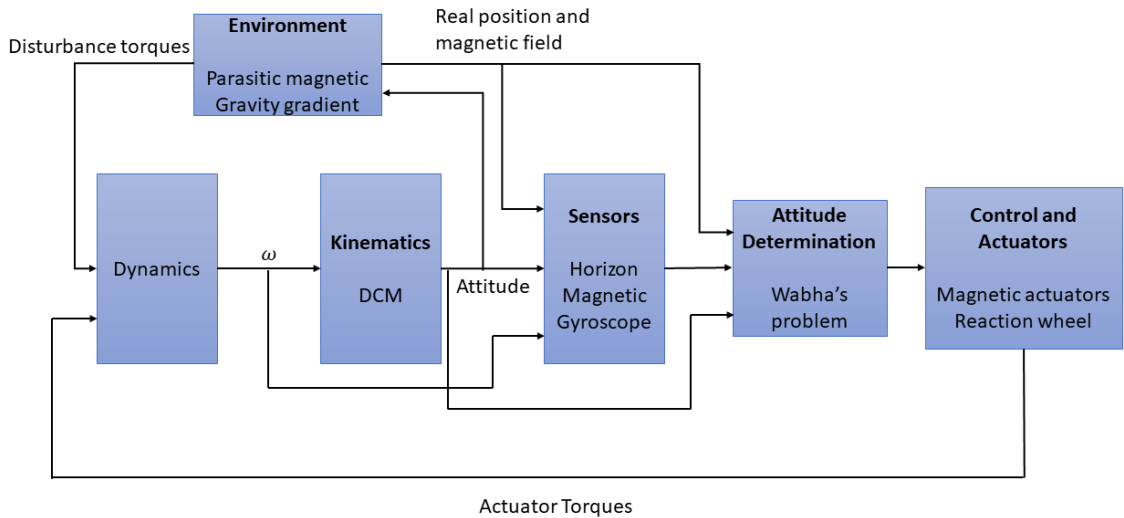


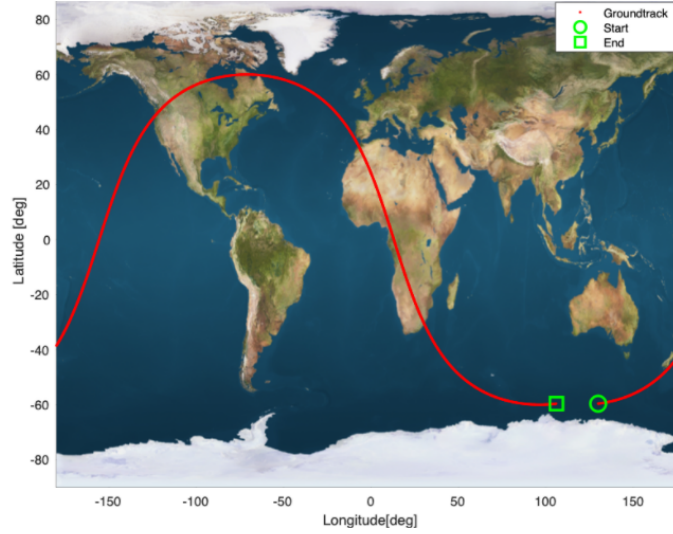
Figure 1.1: ADCS sketch

## 1.2 Orbit characterization

Since the main goal of the mission is to perform the observation of an area on the surface of the earth, it's convenient to inject the 12U cubesat into a Low Earth Orbit, which keplerian elements are shown in the following chart.

The orbit is chosen properly to have Earth's surface coverage in the Pacific Ocean region where the pacific garbage patch is located, in the west zone of North America.

a [km]	inc [deg]	e [-]	RAAN [deg]	$\omega$ [deg]	$\theta_0$ [deg]
6.900	1.0472	0.05	3.6652	0.7854	0

**Table 1.1:** Orbital elements

### 1.3 Spacecraft properties

The spacecraft is a 12U cubesat, with the following dimensions: 240 mm  $\times$  230 mm  $\times$  360 mm. The satellite is assumed to have a homogeneous mass distribution, with a total mass of 12 kg. This will give the moment of inertia for the spacecraft:

$$J = \begin{bmatrix} 0.1825 & 0 & 0 \\ 0 & 0.1872 & 0 \\ 0 & 0 & 0.1105 \end{bmatrix} \text{ kg m}^2 \quad (1.1)$$

The purpose of this cubesat is to assist with ship tracking for Ocean Clean Up crew, therefore the cubesat will be outfitted with a radio receiver. This is directional and will require the cubesat to perform nadir pointing with a pointing accuracy of 5° for the pitch axis. There is no operational requirement for the two remaining axis but a requirement of 5° has been imposed as well.

A sketch of the 12 U cubesat can be seen on figure 1.2 on the following page, along with its body frame.

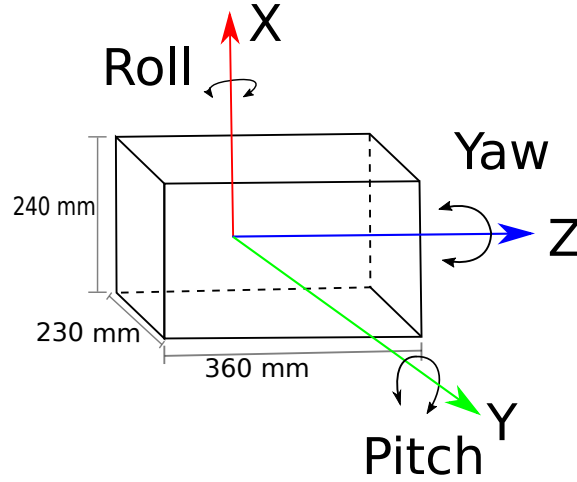


Figure 1.2: 12U CubeSat and body frame

## 1.4 Environment

Since the spacecraft is held within the environment, it is necessary to consider that, according to its position with respect to the Earth and its dimensions, some external factors can modify its performances through the action of moments they are able to generate upon it. It's crucial to detect the most significant ones, which in this case of a Cubesat in a LEO (low Earth orbit) can be identified as the Gravity Gradient torque and the Parasitic Magnetic torque, due to the magnetic field naturally generated by the earth, as we will see from the equation of the dynamics, which expressions can be summarized as

$$\underline{M} = \underline{m} \times \underline{b}$$

PARASITIC MAGNETIC TORQUE

$$M = \frac{3Gm_t}{R^3} \begin{Bmatrix} (I_z - I_y)c_2c_3 \\ (I_x - I_z)c_1c_3 \\ (I_y - I_x)c_1c_2 \end{Bmatrix}$$

GRAVITY GRADIENT TORQUE

Both of them are computed in the body frame. Regarding the parasitic magnetic torque, it's needed to underline that the model which has been used is the Simple dipole model ( $n=1$ ), which allow us to compute the magnetic field vector, computed through the following equations, by taking into account some data taken from the following chart, with a simplified model that implies less accuracy. Anyway, it's noteworthy to say that the further we go from the earth, the better this approximation is, since the magnetic field gets smaller.

$$\underline{b}_N = \frac{R^3 H_0}{r^3} [3(\underline{\hat{m}} \cdot \underline{\hat{r}})\underline{\hat{r}} - \underline{\hat{m}}]$$

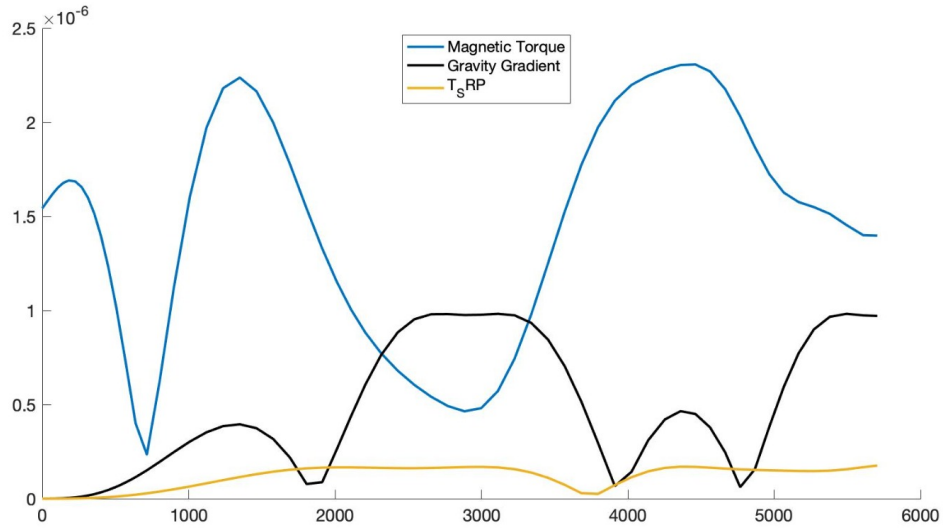
$$H_0 = \left( (g_1^0)^2 + (g_1^1)^2 + (h_1^1)^2 \right)^{1/2}$$

$$\underline{\hat{m}} = \begin{bmatrix} \sin 11.5^\circ \cos \omega_\oplus t \\ \sin 11.5^\circ \sin \omega_\oplus t \\ \cos 11.5^\circ \end{bmatrix}$$

$$\underline{b}_B = A_{B/N} \underline{b}_N$$

		IGRF 1995		IGRF 2000	
n	m	$g_n^m$	$h_n^m$	$g_n^m$	$h_n^m$
1	0	-29682	-	-29615	-
1	1	-1789	5318	-1728	5186
2	0	-2197	-	-2267	-
2	1	3074	-2356	3072	-2478
2	2	1685	-425	1672	-458
3	0	1329	-	1341	-
3	1	-2268	-263	-2290	-227
3	2	1249	302	1253	296
3	3	769	-406	715	-492
4	0	941	-	935	-
4	1	782	262	787	272
4	2	291	-232	251	-232
4	3	-421	98	-405	119
4	4	116	-301	110	-304

There are two other important disturbances as well, which are known as Solar Radiation pressure and force due to Air Drag, both related to the surfaces of the body, which can be discarded since their effects are not relevant compared to the previous ones, considering the limited dimension of a 12U Cubesat. The comparison among the disturbances is shown below.



## 1.5 Dynamics

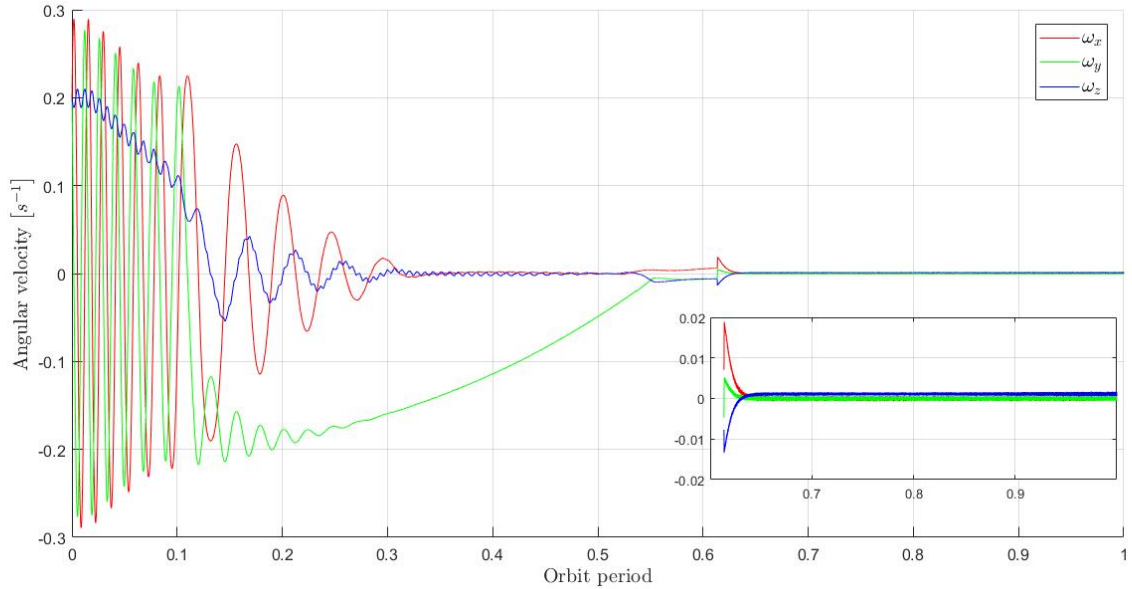
The dynamics has been studied by integrating the Euler equations and considering the presence of an inertia wheel, control moments and the disturbance torques on the right hand side of the following relation

$$J \dot{\omega} + \omega \times (I \omega) + \omega \times h_r + \dot{h}_r = M_d + M_C \quad (1.2)$$

Isolated for  $\dot{\omega}$ :

$$\dot{\omega} = \left( M_d + M_C + (I \omega) \times \omega + h_r \times \omega - \dot{h}_r \right) J^{-1} \quad (1.3)$$

The following graphs, show the behaviour of the components of the angular velocities along the three different axis.



## 1.6 Kinematics

The assigned kinematics is the direction cosine matrix which is defined as the following:

$$\frac{dA_{B/N}(t)}{dt} = - \begin{bmatrix} 0 & -\omega_3 & \omega_2 \\ \omega_3 & 0 & -\omega_1 \\ -\omega_2 & \omega_1 & 0 \end{bmatrix} A_{B/N}(t) \quad (1.4)$$

Using the angular velocities from the dynamics, the kinematics can be updated. Due to the numerical integration the A matrix will no longer be orthogonal after a certain number of integration steps. To orthogonalize A with a first order approximation, during the simulation, the following formula was used:

$$A_{B/N}(t) = A_{B/N}(t) \frac{3}{2} - A_{B/N}^T(t) \frac{A_{B/N}(t)}{2} \quad (1.5)$$

To accomplish the nadir point a second frame was necessary, using a frame defining the attitude between the inertial and LVLH frame, called  $A_{L/N}$ .

$$A_{L/N} = \begin{bmatrix} \cos(n t) & \sin(n t) & 0 \\ -\sin(n t) & \cos(n t) & 0 \\ 0 & 0 & 1 \end{bmatrix} \quad (1.6)$$

$$n^2 = \frac{G m_{\oplus}}{R^3} \quad (1.7)$$

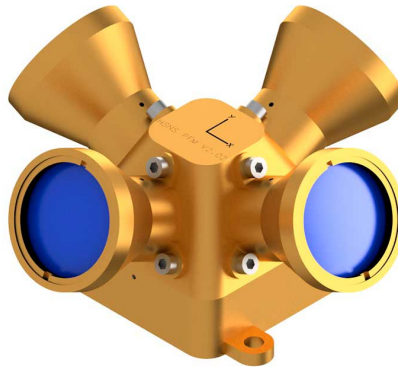
Using the  $A_{L/N}$  frame and the frame defined from the attitude determination, it is possible to formulate an attitude error, e.i. the difference between the satellites body frame and the LVLH frame. This attitude error matrix should become an identity matrix during the slew and tracking phase of the orbit.

## 1.7 Sensors

Sensors are fundamental onboard devices that allow to measure different physical quantities, in order to analyze the space environment. One of the main use is the attitude determination: in order to perform the attitude determination through the sensors we need at least two independent unit vectors, in our case coming from the measurements of the onboard instruments: an horizon sensor and a magnetometer.

### Horizon sensor

The horizon sensor detects the center of Earth giving as output the position vector of Earth in its own reference frame, then converted into the spacecraft's body frame. The behaviour of the sensor is modeled by taking the position vector of the spacecraft along the orbit in the inertial reference frame, and normalizing it. Then it's rotated of 180 degrees in order to obtain a unit vector from the spacecraft to the center of Earth. Like every sensor, it is affected by errors that determine that every measurement has a degree of uncertainty. Typically, horizon sensors work in the infrared wavelength because in this way the noise due to infrared radiation coming from space isn't high comparing to the one coming from Earth. In the case of visible wavelength instead, the ratio between the signal coming from Earth and the signal coming from Sun would be low, so the noise would be higher. Basing our model on the properties of this horizon sensor taken online, we need to consider the accuracy:





Sensor	Accuracy	FOV of each eye	Update Rate
Horizon Sensor	$<1$ [ $^{\circ}$ ]	$\pm 2.5^{\circ}$	10 [Hz]

**Table 1.2:** Horizon sensor specifications satsearch, 2021

The measure is affected by a noise that causes modifications in the output. The error included is a random noise with zero mean and a variance linked to the accuracy of the sensor.

## Magnetometer

A Magnetometer is a sensor that measure the external magnetic field using three pairs of nuclei mutually orthogonal. Unlike the horizon sensor, a magnetometer outputs the vector magnetic field and not the unit vector; in our model we compute the unit vector starting from the magnetic field modeled with the dipole model so the model of the order one, and even if the orbit is not too high, we take into account this approximation. The errors are again added to the signal with a random noise with zero mean and a variance linked to the accuracy of the sensor; typically the errors in the magnetometers are due to orthogonality errors, scale factor and hysteresis.



Sensor	Orthogonality	Update rate	Resolution
Magnetic Sensor	$\pm 1^{\circ}$	$<18$ [Hz]	$<8$ [nT]

**Table 1.3:** Magnetometer specifications. CubeSatShop, 2021d

The two unit vectors computed, are then exploited in the Attitude Determination.

## Gyro

A gyro is a sensor that measures the angular velocities of the spacecraft. The knowledge of the angular velocities is fundamental for the analysis of the mission, in particular we used it for the detumbling and slew-tracking control. The modeling of the behaviour is again computed starting from the angular velocities outputted from dynamics block, and adding a random noise with zero mean. Errors in this type of sensor are defined white noise and rate random walk.



GYRO	Update rate	$\sigma$ ARW	$\sigma$ RRW
STIM 318	262 [Hz]	0.15[deg / $\sqrt{h}$ ]	0.30 [Hz]

**Table 1.4:** Sensor specification. CubeSatShop, 2021b

## 1.8 Actuators

Actuators are the components of a spacecraft that correct or modify the position of the body in space. The characteristics and the behaviour of the actuator depend strictly on the specific actuator. In our case we utilize **magnetic actuator and inertia wheels**; the nature of these two tipologies of actuators is different, since the magnetic actuators determine an effective torque to the spacecraft which implies an external torque in the dynamics equations, while inertia wheels belong to a family of actuators called momentum exchange devices, since their action doesn't consist of a effective torque applied but on an extra contribution in the direction of the axis of the wheel.

Our actuator configuration consists of:

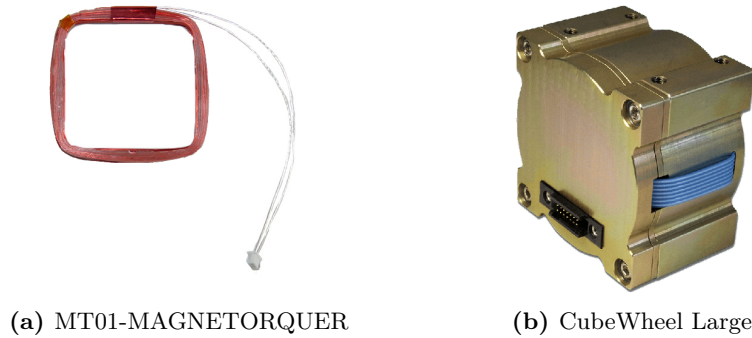


**Figure 1.3**

Actuator	Axis
3 x Magnetic Rods	X
3 x Magnetic Rods	Y
Inertia Wheels Pyramid configuration	XYZ

### Magnetic Actuator

The torque generated by these actuators is:

$$\underline{M} = \underline{D} \times \underline{B} \quad (1.8)$$

Where  $\underline{D}$  is the dipole internally generated and the  $\underline{B}$  is the external magnetic field. We want to achieve what is the actuator action (  $\underline{D}$  vector) from the output of the control block, that is the control moment vector. It can be observed that it's never possible to generate three independent components of the control torque using three orthogonal coils. Then we have used an approximate solution, showed below. We've chosen to put 2 coils along X direction, 2 coils around Y and 2 coils around Y, in this way the control torques are distributed better among the actuators and the dipoles generated are less than the case with less actuators and we can avoid saturation. The saturation is also controlled by a MATLAB function that corrects the magnitude of the dipoles every time

it overcomes the maximum or minimum value of the dipole intensity. The inertia wheels are distributed in a pyramid scheme and also in this case the saturation is controlled such that the wheel never overcomes its range of operation. The magnetic actuators involved have these characteristics:

Actuator	Nominal Magnetic moment	Saturation Moment	Linearity
Magnetotorquer	$< 0.19[Am^2]$	$> 0.85[Am^2]$	$\pm 4\%$ Across operating design range

**Table 1.5:** Magnetotorquer specifications. CubeSatShop, 2021c

The combination of the two actuators is expressed through these equation:

$$\underline{M_C} = \underline{D} \times \underline{B} \quad (1.9)$$

$$\underline{B} \times \underline{M_C} = \underline{B} \times (\underline{D} \times \underline{B}) \quad (1.10)$$

$$\underline{B} \times \underline{M_C} = (\underline{B} \cdot \underline{B})\underline{D} - (\underline{D} \cdot \underline{B})\underline{B} \quad (1.11)$$

We assume that the dipole is always perpendicular to the external field:

$$\underline{D} \cdot \underline{B} = 0 \quad (1.12)$$

$$\underline{B} \times \underline{M_C} = B^2 \underline{D} \quad (1.13)$$

$$\underline{D} = \frac{\underline{B} \times \underline{M_C}}{B^2} \quad (1.14)$$

Then we compute the effective torque, which isn't equal to the control torque because along the orbit the magnetic field changes continuously and it's not orthogonal to the control moment.

$$\underline{M_{eff}} = \frac{1}{B^2} (\underline{B} \times \underline{M_C}) \times \underline{B} \quad (1.15)$$

## Inertia Wheel

The inertia wheel is an actuator based on the deceleration and acceleration of spinning rotor. An inertia wheel has a non-zero nominal angular velocity exchanging angular momentum with the spacecraft. The rate of change of the exchanged angular momentum is:

$$\dot{\underline{h}} = -A^* (\underline{M_C} + \underline{\omega} \times A \underline{h_r}) \quad (1.16)$$

A is a direction cosine matrix that identifies the disposition of the actuators in the spacecraft, while  $A^*$  is its pseudoinverse. We've adopted a pyramid configuration for the wheel, where the actuators have equal components along the principal axes. The A

and  $A^*$  matrices are then computed:

$$A = \begin{bmatrix} -a & a & a & -a \\ -a & -a & a & a \\ a & a & a & a \end{bmatrix} \quad a = \frac{1}{\sqrt{3}} \quad (1.17)$$

$$A^* = \begin{bmatrix} -b & -b & b \\ b & -b & b \\ b & b & b \\ -b & b & b \end{bmatrix} \quad b = \frac{\sqrt{3}}{4} \quad (1.18)$$

The torque is then given as input in the dynamics.

Speed range	Max torque
$\pm 6000$ RPM	2.3 mN m

**Table 1.6:** Reaction wheel specifications. CubeSatShop, 2021a

## 1.9 Control

The satellite has 3 phases, a free motion, detumbling, and slew/tracking phase. The free motion phase does not require any control, as this is done to simulate the separation time from the rocket, this is 100 s long and starts at  $t = 0$  s. The next phase is detumbling the satellite from an initial angular velocity to zero angular velocity, this phase starts at  $t = 100$  s and ends at  $t = 3500$  s. The final phase is the slew and tracking manoeuvre which starts, after the detumbling, at  $t = 3500$  s.

### Attitude determination

In order to give an input to the actuators the S/C main control logic needs some reference parameters that show how far from the desired attitude it is. To compute those parameters the S/C cpu has to determine the real attitude from sensors data. In this case, the two sensors gives as output two vectors, which is the minimum number required to apply the Wabha's problem.

$$J(A) = \frac{1}{2} \sum_{i=1}^N \alpha_i |s_{B_i} - A_{B/N} v_{N_i}|^2 \quad N \geq 2 \quad (1.19)$$

where:

$$s_{B_i}$$

is the unit vector measured by the sensor, in body frame

$$v_{N_i}$$

is the unit vector of the same celestial bodies but referred to ECI frame.

$$\alpha_1 = \frac{1}{6} \quad \alpha_2 = \frac{1}{30} \quad (1.20)$$

Are the weights referred to the horizon sensor and magnetic sensor, inside Wabha's problem they are normalized.

The analytical solution for the problem consists in maximizing the  $J(A)$  function. Through that and some mathematical computations we obtain a simple form to compute the DCM matrix:

$$\begin{aligned} A_{B/N} &= U M V^T; \\ M &= \text{diag}[1 \quad 1 \quad \det(U) \det(V)] \end{aligned} \quad (1.21)$$

U and V have been computed through an singular value decomposition function (svd) applied on matrix B:

$$B = \sum_{i=1}^N \alpha_i s_{B_i} v_{N_i} \quad (1.22)$$

Once computed

$$A_{B/N}$$

, considering that the target attitude is the LVLH frame we get the error matrix:

$$A_e = A_{B/N} A_{L/N}^T \quad (1.23)$$

### Detumbling

The detumbling is done using only the magnetic torque rods. In this configuration the satellite has 9 torque rods in total, which are placed so that there is two on each axis. The spin rate damping is done using active control with only the magnetic actuators. This can be achieved using feedback on the rate of change of the external magnetic field  $B$  on the magnetic torques. This is done using the measured angular velocities from the gyroscope and the measured magnetic field from the magnetic sensor. For high spin rates the rate of change of the magnetic field can be computed as the following, as the change is assumed to be because a high spin rate and not a change in position along the orbit:

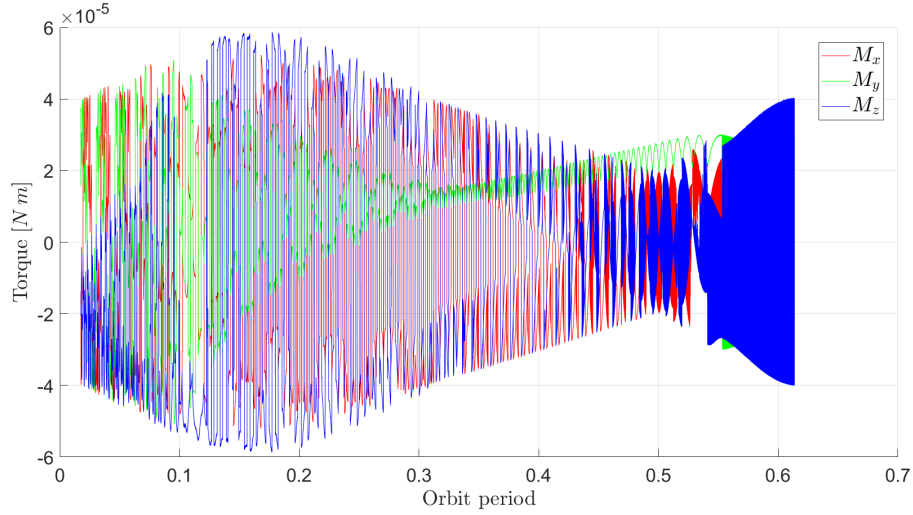
$$\dot{\underline{B}} = -[\omega \times] \underline{B} \quad (1.24)$$

The control equation and gain is the following:

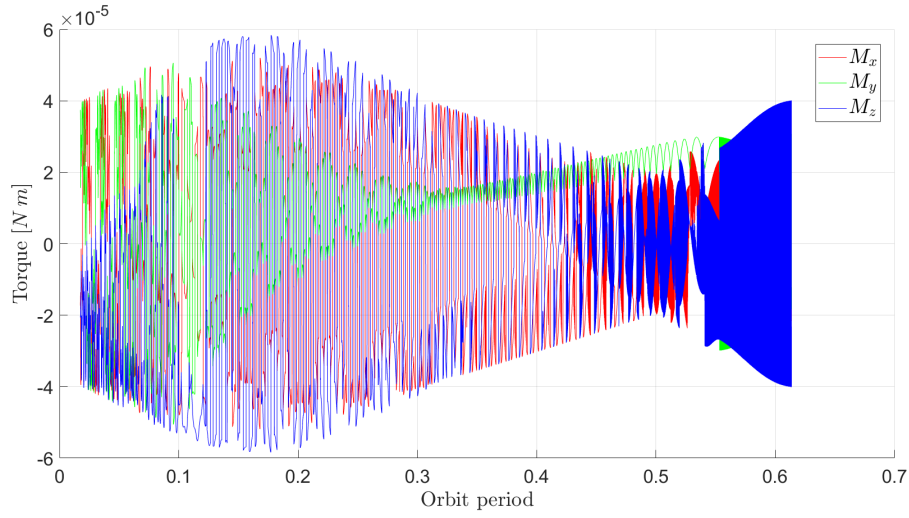
$$k_b = 5 \times 10^8 \quad (1.25)$$

$$\underline{M}_c = -k_b \dot{\underline{B}} \times \underline{B} \quad (1.26)$$

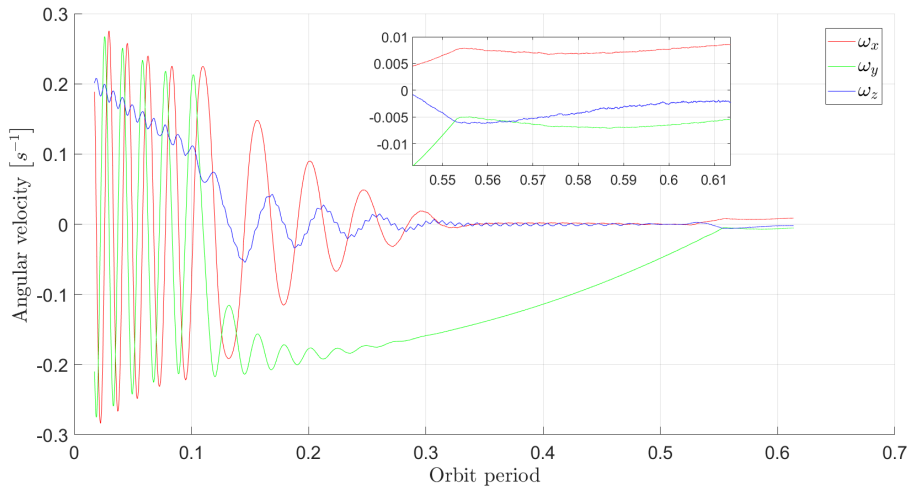
This control is effective when the spin rate is high, in our case the initial angular velocities are  $\omega_0 = [0.2 \ 0.2 \ 0.2]^T$ . As the spacecraft starts to slow down, the applied control law doesn't work anymore. Since the next manoeuvres can be actuated even if the spacecraft isn't fully stopped, there's no need to apply another law and continue the detumbling. Figure 1.4 on the following page shows the magnetic moment and spacecraft detumbling.



(a) Control torques during detumbling phase



(b) Actuator torques during detumbling phase

(c)  $\omega$  during detumbling phase**Figure 1.4:** Detumble phase

### Slew and Tracking maneuver

After detumbling when the spacecraft has reduced the initial velocities, the real mission can start. The spacecraft needs to orient itself towards the earth in order to collect the radio transponder data from the ships, and to relay those data back to a ground-station. This phase is only using the inertia wheels with the pyramid configuration.

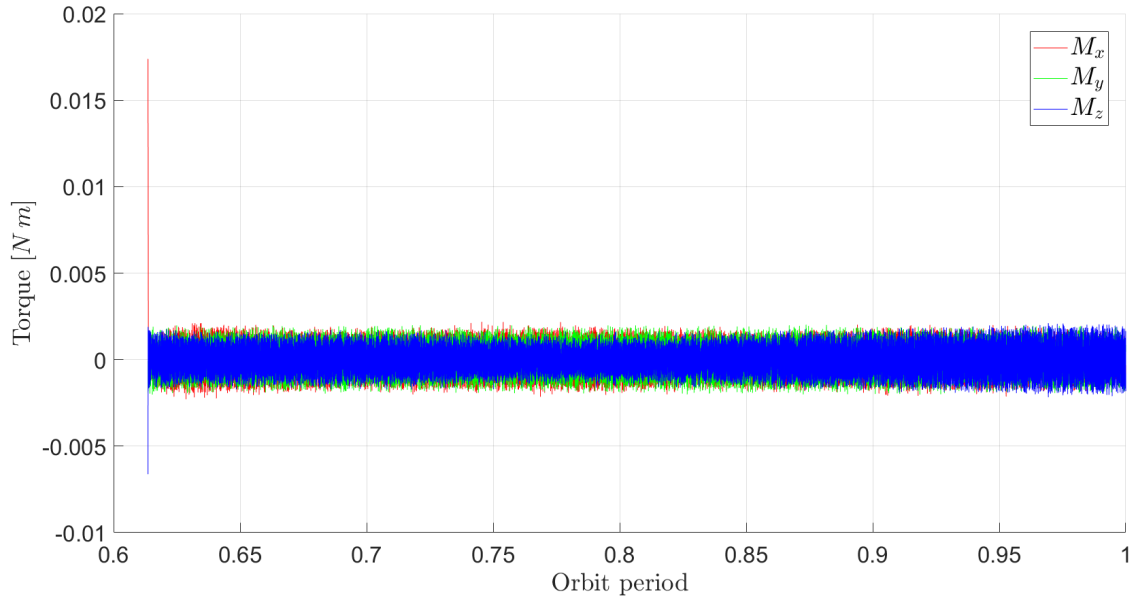
For this phase a non-linear control is implemented using the DCM. The control equation used is:

$$\underline{u} = -k_1 \underline{\omega}_e - k_2 \left( A_e^T - A_e \right)^V + \underline{\omega} \times (J \underline{\omega}) \quad (1.27)$$

After tuning the control, the gains are:

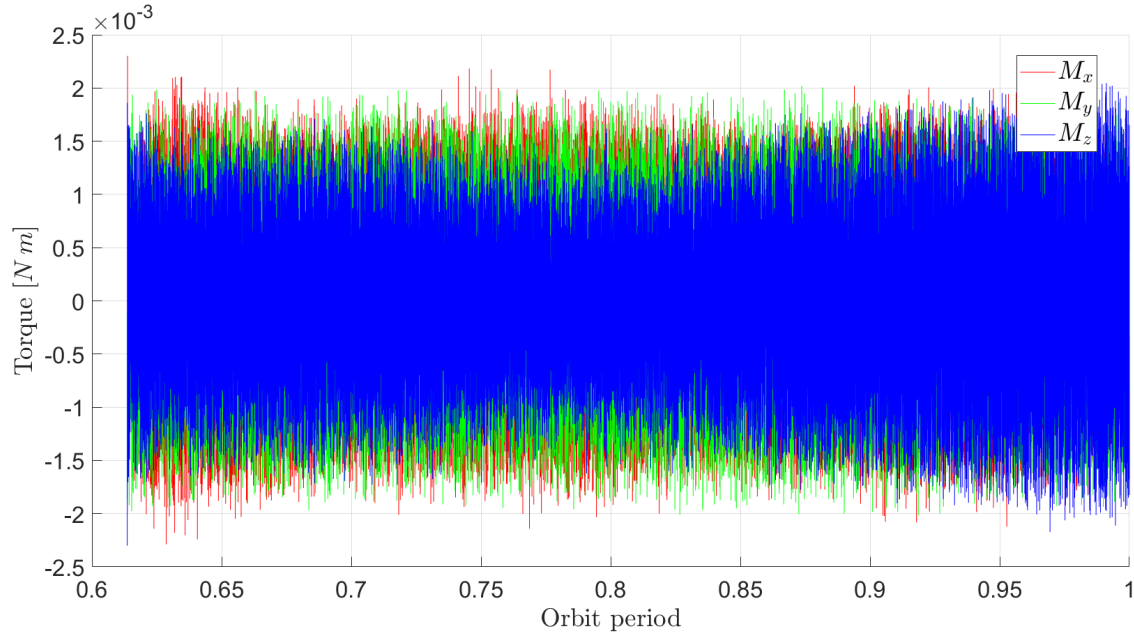
$$k_1 = 1.4 \quad k_2 = 0.02 \quad (1.28)$$

Figure 1.6 shows the ideal torque from the control law, the actual torque given by the reaction wheels and the satellite's angular velocities during the slew/tracking phase.



**Figure 1.5:** Ideal tracking torques

From these figures the slew/tracking manoeuvre takes approximately 1/20 of a orbit period, which is  $\approx 5$  min, to align the satellite with the target frame and start it's main assignment. One could argue that the controls are quite aggressive, the motion could be smooth out so that the change in  $\omega$  is not so violent. This would require further tuning off the control gains or possibly a new control scheme.



**Figure 1.6:** Reaction wheel torques

## 1.10 Control verification

The pointing requirement for the satellite was  $5^\circ$  for each axis. This was used to ensure functionality of the on-board radio. From the previous figures it can be seen that the satellite follows the target frame and performs nadir pointing.

For this control to work the  $A_e$  matrix needs to move towards an identity matrix. In Figure 1.7 the off-diagonal small error angles from the  $A_e$  matrix is shown, the diagonal elements are  $\approx 1$ . Figure 1.8 on the following page show the velocity error between the spacecraft and the target attitude velocity.

In order to confirm the pointing requirement is met the attitude errors have been converted

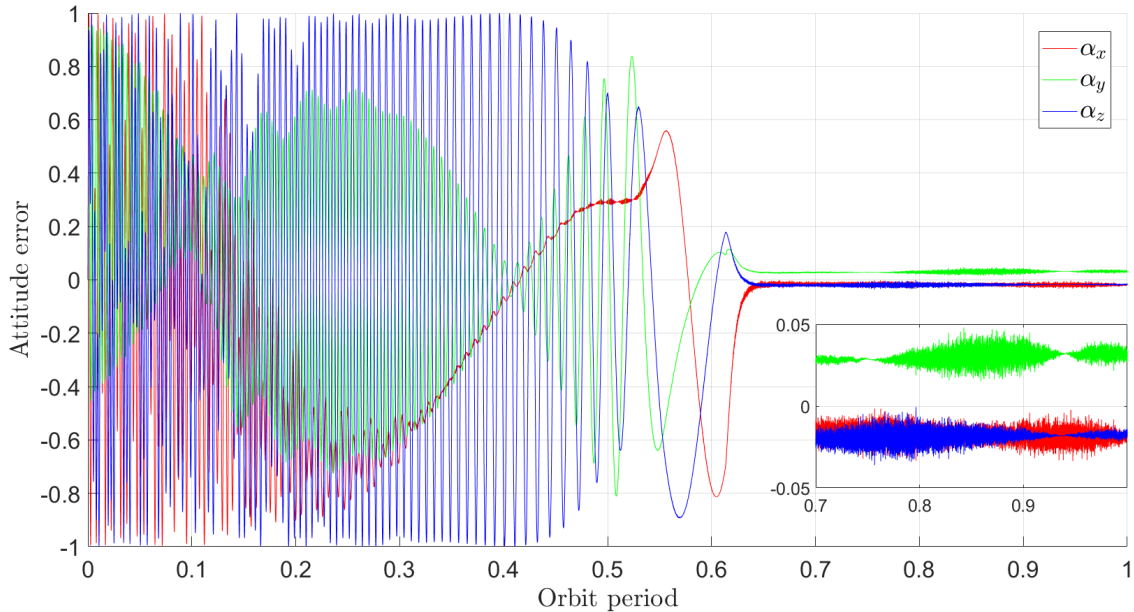


**Figure 1.7:** Tracking errors



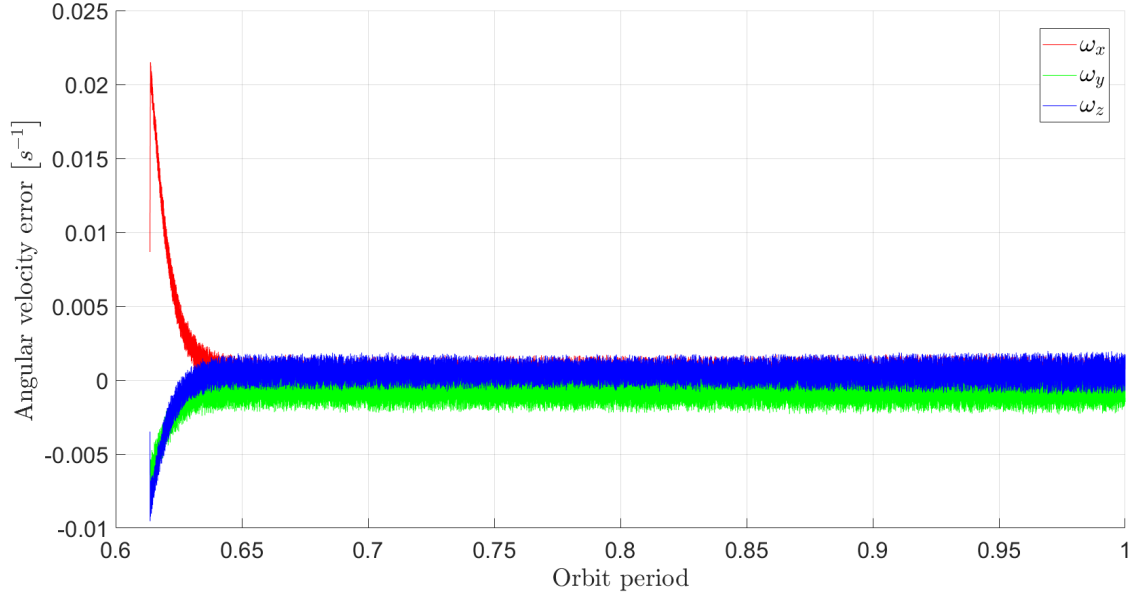


Figure 1.8: Tracking velocities

to Euler angles. The Euler angles error for the 3 phases can be seen on Figure 1.9. It can be seen on this figure that the error angle is  $\approx \pm 2^\circ$

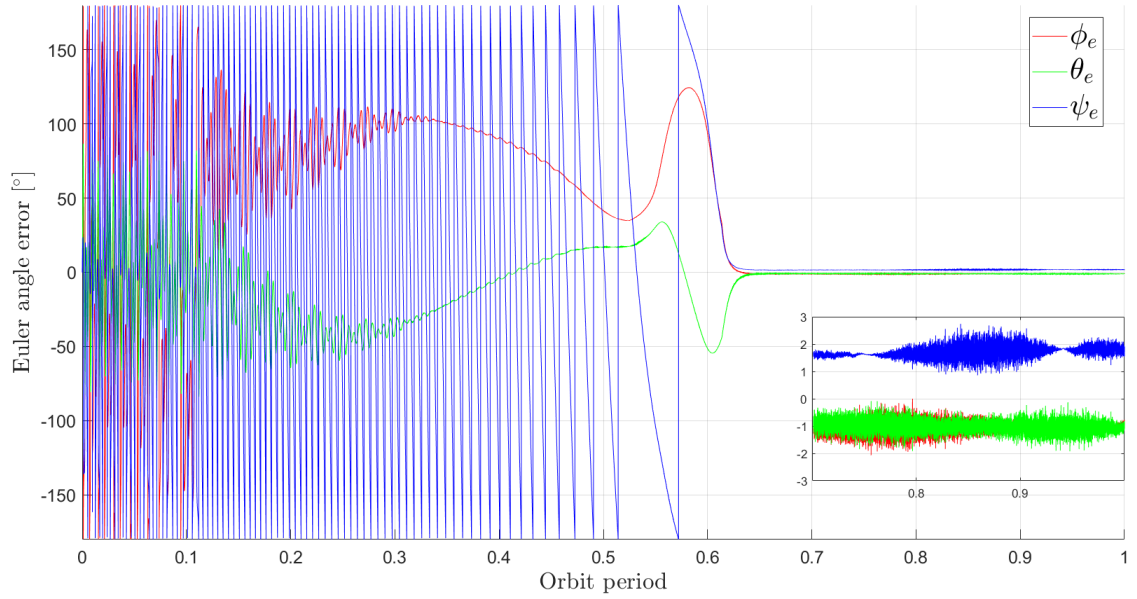


Figure 1.9: Euler angle errors for 1 orbit

Performing a statistical analysis on the three euler angles it is possible to verify if the pointing precision meets the requirements. We have treated each euler angle error individually, computed their mean and standard deviation, as seen below:

$$\begin{array}{ll}
 \overline{\phi_e} = -1.05^\circ & \sigma_{\phi_e} = 0.18 \\
 \overline{\theta_e} = -1^\circ & \sigma_{\theta_e} = 0.22 \\
 \overline{\psi_e} = 1.7^\circ & \sigma_{\psi_e} = 0.19
 \end{array}$$

The results obtained imply that the errors during the pointing phase are densely distributed around the mean values. Considering that the required error is below 5 degrees and that in the worst case one of the Euler angles' error stays still below three, we can say that the control systems works as intended.

### 1.11 Conclusion

The purpose of this project was to develop a Attitude control system for a 12 U cubesat with a mass of 12kg, which should perform nadir pointing in order to receive radio data from ships. The sensors assigned was the horizon and magnetic sensors, though a gyroscope was added because it would increase the accuracy of the control laws. The actuators used on-board the spacecraft was 2 pairs of magnetic torque rods, e.i. 2 rods pr. axis, 4 reaction wheels in a pyramid scheme.

The satellite has 3 phases, a free motion, detumbling, and slew/tracking phases. The detumbling control managed to detumble the satellite from an initial velocity  $\omega_0 = [0.2 \ 0.2 \ 0.2]^T$  to approximately  $[0.008 \ -0.005 \ -0.002]^T$ . The gain for the detumbling control was tuned to  $5 \times 10^8$ .

The slew/tracking control has an error of  $\approx \pm 2^\circ$ , which means that the pointing requirement is met and the satellite will be able to receive radio data. The gains for the slew/tracking control was tuned to  $k_1 = 1.4$  and  $k_2 = 0.02$ .

# Bibliography

---

## Websites

- CubeSatShop (2021a). *CubeWheel Large*. URL: <https://www.cubesatshop.com/product/cubewheel-large/> (visited on 12/21/2021).
- (2021b). *CubeWheel Medium*. URL: <https://www.sensoror.com/products/inertial-measurement-units/stim318/> (visited on 12/21/2021).
  - (2021c). *EXA MT01 Compact Magnetorquer*. URL: <https://www.cubesatshop.com/product/mt01-compact-magnetorquer/> (visited on 12/21/2021).
  - (2021d). *NSS Magnetometer*. URL: <https://www.cubesatshop.com/product/nss-magnetometer/> (visited on 12/21/2021).
- satsearch (2021). *HSNS - Horizon Sensor for Nanosatellites*. URL: <https://www.sensoror.com/products/inertial-measurement-units/stim318/> (visited on 12/21/2021).

